Uncertainty Analysis for a Simplified Characterization of Test Low-Power Voltage Transformers in the 9–150-kHz Frequency Range

Published Version:
Betti, C., Tinarelli, R., Peretto, L., Mingotti, A. (2025). Uncertainty Analysis for a Simplified Characterization of Test Low-Power Voltage Transformers in the 9–150-kHz Frequency Range. IEEE TRANSACTIONS ON INSTRUMENTATION AND MEASUREMENT, 74, 1-8 [10.1109/tim.2025.3569355].

Availability:
This version is available at: https://hdl.handle.net/11585/1017393 since: 2025-06-09

Published:
DOI: http://doi.org/10.1109/tim.2025.3569355

(Article begins on next page)

Conference ID: 62611X

Uncertainty Analysis for a Simplified Characterization of Test Low-Power Voltage Transformers in the 9 kHz to 150 kHz Frequency Range

C. Betti, Student Member, *IEEE*, R. Tinarelli, Senior Member, *IEEE*, L. Peretto, Senior Member, *IEEE*, and A. Mingotti, Member, *IEEE*

***Abstract*—The growing integration of renewable energy sources into national power grids is impacting electricity quality, primarily due to the widespread use of electronic power converters. These converters, which rely on switching components, can introduce high-frequency harmonics, reaching up to 150 kHz, into the grid. However, current international standards and state-of-the-art literature on instrument transformers provide limited guidance on methods, techniques, parameters, and metrological requirements necessary for power quality measurements at frequencies above tens of kilohertz. In response, this paper presents an example of cost-effective measurement setup used to test four medium-voltage low-power instrument transformers within the frequency range of (9 to 150) kHz. A detailed uncertainty analysis is conducted using both standard accuracy indices (ratio error and phase displacement) and less common indices (composite error). Lastly, the paper discusses an approach to the uncertainty evaluation for high-frequency components. The results demonstrate the method's applicability, replicability, and value for end-users.**

***Index Terms*— Low-power Voltage Transformers, Power Quality, Uncertainty evaluation, Accuracy, Medium Voltage, Frequency Characterization**

I. INTRODUCTION

THE previous model of electric power network characterized by (i) centralization of power generation, (ii) unidirectional energy flows and (iii) a strong prevalence of non-renewable forms of energy is being replaced by the future model called smart grid. Smart grids are based on distributed generation with the presence of bidirectional power flows and an important percentage of renewable energy sources. Despite the numerous benefits of this new type of infrastructure, the problem of power quality (PQ) degradation is becoming non-negligible, because, to feed energy into the grid, green energies need power electronic converters which are among the causes of PQ worsening [1]. Therefore, the international context of growing energy demand, combined with the need to reduce environmental impact, is pushing the integration of renewable energy sources at all voltage levels and particularly in the MV one. Consequently, the disturbances caused by power converters are putting the stability of electrical systems under pressure, because, due to the high frequency switching of electronic components, this type of converter can inject harmonics up to 150 kHz into the network [2]. In general, the presence of harmonics is the cause of (i) overheating of components, (ii) power losses, (iii) failure of electronic components, (iv) intervention of protections and many other unwanted events that lead to economic losses and reduced safety [3,4]. Reliable PQ measurements are essential for accurately assessing network conditions and preventing faults. Inaccurate measurements increase the risk of undesirable events. As instrument transformers (ITs) are widely used for current and voltage measurements in MV networks, understanding their performance at higher frequencies has become an active area of research.

Within the academic community, the study of the characterization of MV ITs with respect to frequency has been prolific. For example, in 50 Hz systems, the traditional PQ band up to 2.5 kHz is addressed in many works and using different types of devices: (i) inductive current transformer [5, 6], (ii) conventional voltage transformer [7, 8], and finally low-power instrument transformers (LPITs) [9, 10]. However, the accuracy of MV ITs vs. frequency over the extended frequency range from 2 kHz to 150 kHz is less investigated. At the international level, the EURAMET project 19NRM05 IT4PQ [11] focused on establishing new accuracy limits, parameters, and testing methods for PQ measurements of currents and voltages up to 9 kHz in MV ITs. One goal of IT4PQ was to support IEC Technical Committee 38 in updating current standards. Following IT4PQ, the EURAMET project 22NRM06 ADMIT [12] aims to further extend the analysis range, raising the upper measurement limit from 9 kHz to 150 kHz.

This paper is the technical extension of [13], which introduced a simplified and low-cost harmonic characterization method for MV low-power voltage transformers (LPVTs) in the 9 kHz to 150 kHz range. The method included a low-cost setup, which can be substituted by any other ones, and the injection of

C. Betti, R. Tinarelli, L. Peretto, and A. Mingotti are with University of Bologna, Department of Electrical, Electronic and Information Engineering "Guglielmo Marconi" Alma Mater Studiorum - University of Bologna Bologna, 40136, Italy. christian.betti2, roberto.tinarelli3, lorenzo.peretto, alessandro.mingotti2@unibo.it.

TABLE I. RATIO ERROR AND PHASE ERROR LIMITS TAKEN FROM [16]

Accuracy class	WB	Ratio Error (%)			Phase Error (°)		
	WB1	fr < f ≤ 1 kHz	1 < f ≤ 1.5 kHz	1.5 < f ≤ 3 kHz	fr < f ≤ 1 kHz	1 < f ≤ 1.5 kHz	1.5 < f ≤ 3 kHz
	WB2	fr < f ≤ 5 kHz	5 < f ≤ 10 kHz	10 < f ≤ 20 kHz	fr < f ≤ 5 kHz	5 < f ≤ 10 kHz	10 < f ≤ 20 kHz
	WB3	fr < f ≤ 20 kHz	20 < f ≤ 50 kHz	50 < f ≤ 150 kHz	fr < f ≤ 20 kHz	20 < f ≤ 50 kHz	50 < f ≤ 150 kHz
	WB4	fr < f ≤ 50 kHz	50 < f ≤ 150 kHz	150 < f ≤ 500 kHz	fr < f ≤ 50 kHz	50 < f ≤ 150 kHz	150 < f ≤ 500 kHz
0.1		±1	±2	±5	±1	±2	±5
0.2 - 0.2 S		±2	±4	±5	±2	±4	±5
0.5 - 0.5 S		±5	±10	±10	±5	±10	±20
1		±10	±20	±20	±10	±20	±20
Protection		±10	±20	±30	–	–	–

specifically designed signal. Such a signal is based on a sinc signal, and it was introduced by the authors in previous publications [14]. Here, the setup is applied to test four LPVTs from different manufacturers to confirm the approach's broader applicability. The main contributions of this paper include: (i) two additional test devices, (ii) a detailed analysis of phase displacement, complementing the prior discussion on ratio and composite errors from [13], and (iii) comprehensive assessment of the uncertainty evaluation of the high-frequency LPVT characterization. This evaluation is both straightforward to implement and sufficiently accurate to produce reliable results. As detailed in Section II, not many works deal with such an uncertainty evaluation in this complicate frequency range. Furthermore, none includes the use of the sinc signal. Hence, the paper cannot provide any comparison with existing literature.

The rest of the paper is organized as follows. Section II presents to the reader the framework in which the paper is developed. Then, Section III summarizes the description of the "sinc-approach" and measurement setup. Finally, Sections IV and V report experimental results and conclusion, respectively.

II. Scenario

A. Low-power instrument transformers

Low-power instrument transformers (LPITs) were developed to address the limitations of traditional iron-core transformers, particularly for the demands of modern smart grids. LPITs offer advantages in MV applications, including output voltage compatibility with intelligent devices, wide frequency response due to the absence of a ferromagnetic core, smaller size, and lighter weight for easier installation [15]. However, LPITs have some drawbacks, such as high sensitivity to influence quantities like temperature, vibrations, and magnetic fields [9,16].

B. The 9 kHz – 150 kHz frequency range

Supported by the ADMIT project, this work focuses on the frequency range of (9 to 150) kHz—a range lacking international standards for MV equipment, tests, and accuracy requirements. Existing standards for ITs, like IEC 61869, specified accuracy limits only up to the 50th harmonic for AC and 20 kHz for DC applications until the recently published new IEC 61869-1 of 2023 [17]. The document includes a new accuracy class extension for harmonics, aiming to provide a brief indication of the performance of a device in terms of harmonic response. The contribution is given in the form of five wide bandwidth (WB) class WB: (i) WB0, up to 13th harmonic, (ii) WB1, up to 3 kHz, (iii) WB2, up to 20 kHz, (iv) WB3, up to 150 kHz and finally (v) WB4, up to 500 kHz.

These extensions will be added to the accuracy class indication of any device (e.g. 0.5 – WB4). LPITs are requested to be at least WB0. Finally, the IEC 61869-1 set the limits for every accuracy class and for every WB, according to Table I [17]. In detail, for every WB there are three frequency ranges for which limits of ratio and phase error are defined. Note that, as specified in IEC 61869-99 [18] the ratio and phase error are calculated at the fundamental frequency component (50 Hz or 60 Hz).

In other documents like IEC 61869-103 [19] there are technical guidelines for PQ measurements, but specific accuracy classes remain undefined. Likewise, the IEC 61000 standards on electromagnetic compatibility (IEC 61000-4-7 [20] and -4-30 [21]) don't address accuracy for MV transducers. IEEE 519 [22] and IEC 50160 [23] set limits on harmonic emissions up to the 50th harmonic but do not extend beyond. Recent research has begun addressing MV transducer behavior up to 150 kHz, with studies like [24] focusing on harmonic measurements up to 9 kHz and [25, 26] exploring higher frequencies. Overall, researchers are working to bridge these gaps by proposing standardized guidelines for improved asset management in MV systems.

III. Sinc-Approach

A. Method Overview

The theory behind the "sinc-approach" is detailed in [14, 27], and a summary is provided here. First, the sinc testing signal is designed by considering three key parameters: (i) the waveform's sample count based on the arbitrary waveform generator (AWG) memory, (ii) the waveform's frequency resolution, and (iii) the spectrum's cut-off frequency. The spectrum of the sinc function, centered on zero, has a rectangular shape with a specified cut-off frequency. Next, a Blackman window is applied to reduce spectral leakage from signal truncation. The resulting windowed sinc signal (WSS) contains 8192 samples, with a period of 0.5 ms and frequency content up to 150 kHz. Finally, the WSS is applied to the device under test to capture its frequency response, known as the sinc response (SR), covering a frequency range in one measurement. This approach is more efficient (fore some applications) than other traditional methods such as: (i) the frequency sweep, which require several measurements equal to the number of frequencies under test and therefore can be more time-consuming and (ii) the impulse response, which require expensive instrumentation in order to obtain a shape of the impulse as ideal as possible. In conclusion, the main value of [13], in which more details can be found, lies in combining the sinc-approach with a low-cost measurement setup to characterize LPVTs in the (9 to 150) kHz range in a single test, an area not yet standardized.

B. Measurement setup

The measurement setup adopted in this work is represented by the block diagram in Fig. 1. It consists of: (i) two AWGs Rigol DG1022Z with a frequency resolution of 1 μHz, (ii) a precision operational amplifier ADHV4702-1 included in its evaluation board, which has a wide range of operating voltages up to ±105 V (Table II summarizes the main features of the OP-AMP), (iii) four LPVTs (Table III reports the main characteristics of the devices under test) and finally (iv) an oscilloscope Tektronix MSO58

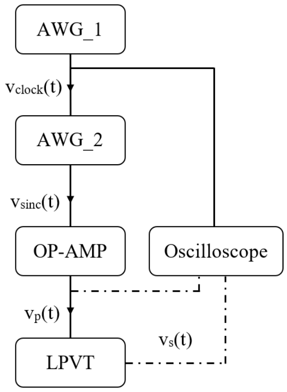

Fig. 1. Block diagram of the measurement setup

TABLE II. MAIN FEATURES OF THE OP-AMP

Dual supply	±12 V to ±110 V	**CMRR**	160 dB
Slew rate	24 V/µs	**Input bias current**	2 pA
Bandwidth	10 MHz	**Input offset voltage**	1 mV

TABLE III. MAIN CHARACTERISTICS OF THE LPVTS

	LPVT 1	**LPVT 2**	**LPVT 3**	**LPVT 4**
Technology	*Passive capacitive*	*Active closed loop fluxgate*	*Passive capacitive*	*Passive capacitive*
Transformation ratio [-]	5981	100	720	8200
Primary voltage [kV]	30	1	20/√(3)	20/√(3)
Accuracy class [-]	0.2	0.2	0.5	0.5

TABLE IV. MAIN CHARACTERISTICS OF THE OSCILLOSCOPE

Vertical division	10	**Maximum V/div setting**	10 V/div
Input impedance	1 MΩ with 13 pF	**Maximum sampling frequency**	6.25 GSa/s
Maximum input voltage	300 V_{RMS}	**ADC resolution**	16 bits

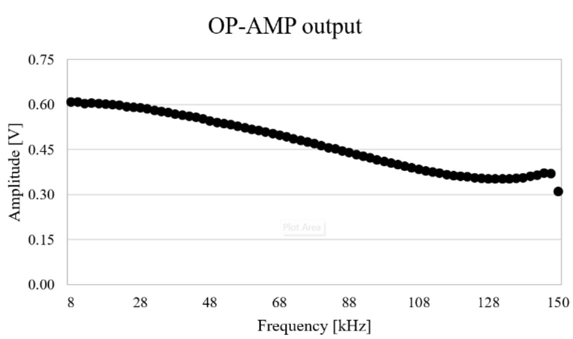

Fig. 2. Amplitude spectrum of OP-AMP output

(Table IV summarizes the main features of the oscilloscope). In a nutshell, AWG_1 provides an external clock reference signal $v_{clock}(t)$ to AWG_2 and oscilloscope. This voltage is a 10 MHz square wave used to synchronize the generation and the acquisition of the measurement chain. Then, AWG_2 generates the designed WSS $v_{sinc}(t)$, which is then amplified by the OP-AMP and applied to the LPVTs under test. Finally, the oscilloscope acquires the primary voltage $v_p(t)$ applied to the device under test and its secondary output voltage $v_s(t)$.

C. Description of the tests

The proposed method collects the sinc response of LPVTs starting from the design of a voltage waveform with a period of 0.5 ms and a frequency spectrum up to 150 kHz, as outlined in IEC 61000-4-30 Annex C [21]. The signal, generated by the AWG and amplified by an OP-AMP, is applied to the LPVTs. Input and output signals are then recorded via oscilloscope and stored on a PC, with 100 repeated measurements capturing 10 cycles each. Using a fast Fourier transform (FFT) over one period, a frequency spectrum with 2 kHz resolution is produced, covering from (8 to 150) kHz. On the signal generation side, the OP-AMP's slew rate limitation reduces amplitude at higher harmonics, which complicates its frequency characterization given the multi-tone nature of the sinc signal. Thus, the OP-AMP output is directly acquired by the oscilloscope, with the sinc function peaking around 75 V (see Fig. 2 and 11), ensuring accurate sampling as demonstrated in a previous work of the authors [27]. Regarding the oscilloscope setup, the vertical settings of each channel are adjusted separately during the tests to optimize the resolution of the ADC. The sampling frequency is set to 5 MSa/s corresponding to a bandwidth equal to 2 MHz.

IV. RESULTS

To assess the experimental results, for each harmonic components of interest, the ratio error, phase displacement and composite error are calculated according to the following equations:

$$\varepsilon_h(\%) = \frac{K_r U_{s,h} - U_{p,h}}{U_{p,h}} * 100 \quad (1)$$

$$\Delta\varphi_h = \varphi_{s,h} - \varphi_{p,h} \quad (2)$$

$$\varepsilon_c(\%) = \frac{\sqrt{\frac{1}{N}\sum(K_r u_s[n] - u_p[n])^2}}{U_p} * 100 \quad (3)$$

The three formulas include the following parameters: (i) the rated transformation ratio K_r of the LPVTs under test, (ii) the rms harmonic components of order h of the primary and secondary, $U_{p,h}$ and $U_{s,h}$, respectively, (iii) the phase of the harmonic component of order h of the primary and secondary signal, $\varphi_{p,h}$ and $\varphi_{p,h}$, respectively, (iv) the total number of considered samples N, (v) the sequence of samples of the primary and secondary, $u_p[n]$ and $u_s[n]$, respectively and finally (vi) the rms value of the primary voltage U_p. In this work, the primary signal is derived from the OP-AMP output, while the secondary signal originates from the LPVTs under test. Notably, the composite error is presented in discrete form in the time domain, whereas its more commonly cited definition, such as in [14], uses an integral representation suited for continuous time-domain signals. This accuracy parameter combines both the amplitude and phase variations of the two waveforms under test, making it a more direct index compared to the traditional ratio error, which accounts only for amplitude differences. Consequently, although the composite error is primarily defined and applied for current transformers, it is introduced here to evaluate the accuracy of LPVTs across this extended

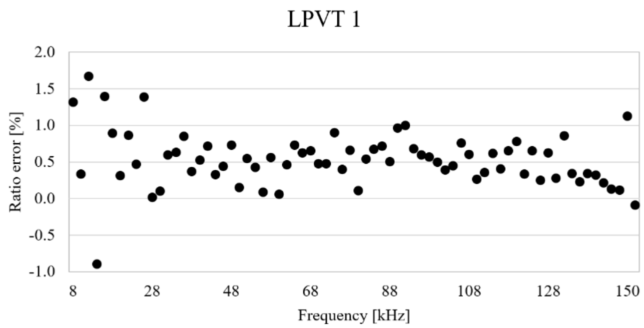

Fig. 3. Ratio error vs. frequency of LPVT 1

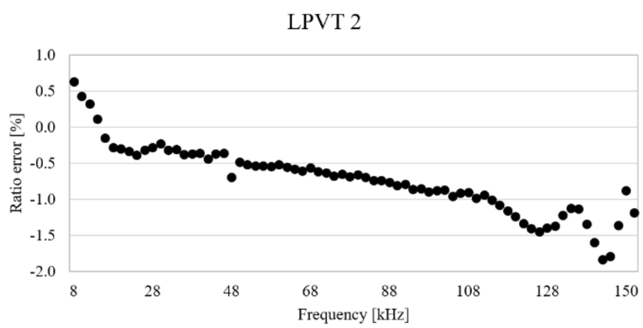

Fig. 4. Ratio error vs. frequency of LPVT 2

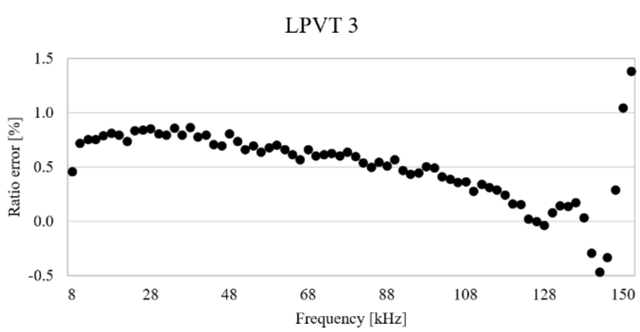

Fig. 5. Ratio error vs. frequency of LPVT 3

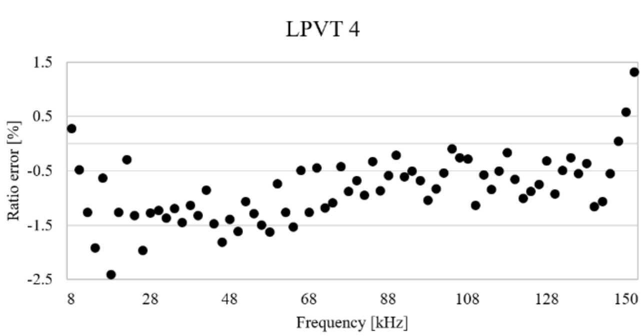

Fig. 6. Ratio error vs. frequency of LPVT 4

frequency range. All the obtained results are presented: (i) in Fig. 3 – 6 for the ratio error, (ii) in Fig. 7 – 10 for the phase displacement, and finally (iii) in Table V for the composite error. In detail, Fig. 3 – 10 shows how the ratio error and phase

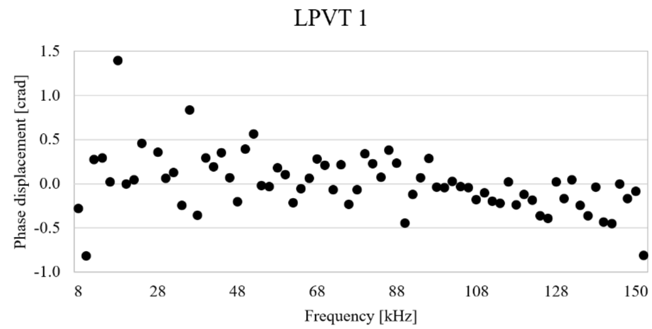

Fig. 7. Phase displacement vs. frequency of LPVT 1

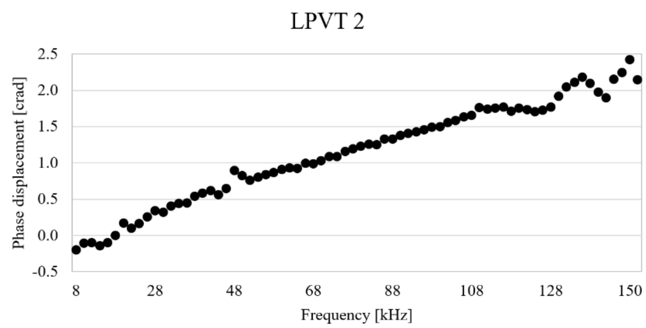

Fig. 8. Phase displacement vs. frequency of LPVT 2

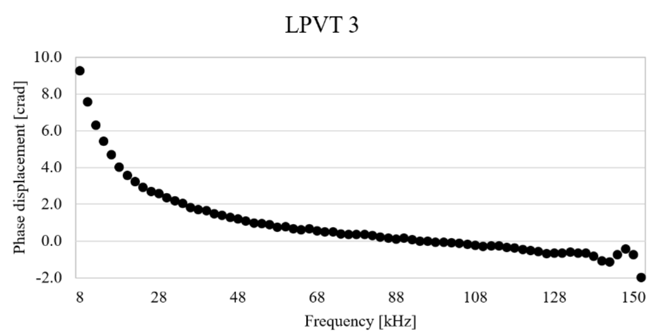

Fig. 9. Phase displacement vs. frequency of LPVT 3

TABLE V. COMPOSITE ERROR OF LPVTS UNDER TEST

	LPVT 1	LPVT 2	LPVT 3	LPVT 4
ε_c(%)	7	6	9	14

displacement of the four LPVTs under test varies with respect to the frequency. As suggested in the Annex C of the IEC 61000-4-30 [25], the x-axis frequency step is equal to 2 kHz. Table V reports the obtained values of the composite error. All values are calculated as the average of the 100 measurements performed during each acquisition.

For the four LPVTs, it can be observed from Fig. 3 – 6 that the ratio error never exceeds ±2 %. In fact, considering the accuracy limits in Table I, the obtained results are included in all the WB for both types of devices tested (accuracy class 0.2 and 0.5). However, the trend over frequency is different. In particular, the behavior of LPVT 1, expressed in percentage, is

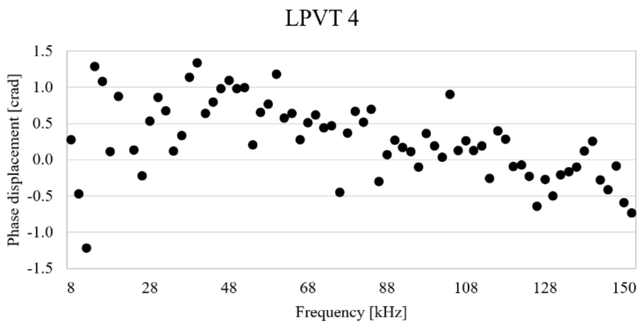

Fig. 10. Phase displacement vs. frequency of LPVT 4

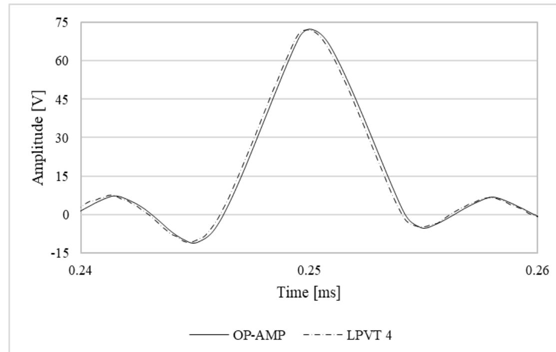

Fig. 11. Amplitude spectrum of OP-AMP and LPVT 4 outputs

mostly random at lower frequencies and tends to stabilize and be more consistent at higher frequencies. While the ratio error of LPVT 2 and 3 show a steady negative drift as the frequency increases with a marked degradation at higher frequencies (> 120 kHz). Finally, LPVT 4 displays a more unpredictable and less stable behavior across the entire frequency range and the ratio error is more pronounced to other three DUTs. Overall, the focus is not on the trend of the accuracy indices, but on their value and the accuracy with which they are obtained. In fact, the method must be replicable, independently of the type of transformer under test.

Observing the phase displacements, for the four LPVTs, it can be observed from Fig. 7 – 10 that it never exceeds 10 crad (0.57°). Therefore, the achieved accuracy is remarkable as already seen for the ratio error. In fact, once again, all the obtained phase displacements are included in the limits of Table I for all WB. The phase displacement over frequency of the four DUTs exhibits different behavior. LPVT 1 shows a stable and random phase performance across the entire frequency spectrum. While LPVT 2 and 3 have a strong frequency-dependent phase displacement. In particular, the first of the two has a linear trend that consistently increases with the frequency while the second of the two tends to decrease exponentially and stabilize as the frequency increases. Finally, LPVT 4, similarly to LPVT 1, demonstrates unpredictable phase behavior. Such behaviors are intrinsic of the type of device tested, but still not the focus of the paper nor it affects the discussion and the results.

To conclude this section, the idea behind Table V is to introduce the composite error as an index that can improve the knowledge of the metrological performance of the devices under test, since the standards are more oriented toward using only the ratio error and phase displacement. Due to the novel use of this index, the values in Table V cannot be compared with standards. However, the obtained percentages are coherent with the distortions included in the waveforms and the physical meaning of the index. To support Table V, Fig. 11 exhibits a portion of the output signal acquired from the OP-AMP and LPVT 4; the latter multiplied by the respective transformation ratio. Therefore, the moderate mismatch between LPVTs input-output can be appreciated in the case of the major composite error among all the devices under test.

V. Uncertainty Evaluation

This section focuses on enhancing the characterization by quantifying the uncertainties associated with the measurements. This evaluation process, also known as "uncertainty propagation", is performed with the support of the Monte Carlo Method (MCM) described in Supplement 1 of the GUM [28]. By identifying the sources of uncertainty, this approach determines the coverage intervals associated with the measurement results. In particular, the MCM method is employed to include the uncertainty associated with the Type B evaluation method. Therefore, after considering the main accuracy parameters of the used oscilloscope and their contribution to uncertainty, this method, allows to obtain the coverage intervals associated with the quantity of interest. Subsequently, these coverage intervals are compared with those obtained using merely the type A uncertainty, i.e. the standard deviations of the results of Fig. 3 – 8, which have an order of magnitude of approximately 0.5 for LPVT 1 and LPVT 4 and 0.05 for LPVT 2 and 3, for both error ratio and phase displacement, with slight variation along the frequency range (which is not the focus of the work and therefore the values are not reported).

A. Bandwidth considerations

The bandwidth (BW) of an oscilloscope is a critical parameter that needs to be considered to accurately acquire the waveform under analysis. In particular, the BW specifies up to what frequency the signal can be measured with acceptable attenuation which is usually defined as a signal reduction of -3 dB [29]. In this study, a signal with a frequency content of 150 kHz is sampled using an oscilloscope with a bandwidth of 2 MHz. Taking this information into account, the attenuation of the signal, caused by the oscilloscope, is calculated assuming that the low-pass frequency response of the oscilloscope is a single-pole Gaussian model. This frequency response shape assumption is conservative in evaluating the signal attenuation caused by the oscilloscope compared to other response shapes, such as the maximally flat response, as this behavior causes a greater attenuation of the frequencies in the band. In addition, this hypothesis is often true for many oscilloscopes below 1 GHz bandwidth [30]. Eq. 4 shows the typical transfer function of a Gaussian frequency response in which f_c is the cut-off frequency (i.e. the bandwidth of the oscilloscope in this paper).

In conclusion, the attenuation at 150 kHz is found to be negligible, with a gain of approximately 99.7 % and an

TABLE VI. ACCURACY PARAMETERS OF THE OSCILLOSCOPE

Reading Error [%]	Full-Scale Error [%]	Noise [mV]
1	0.5	64.8×10^{-3} to 5.47

TABLE VII. VERTICAL SETTINGS OF THE OSCILLOSCOPE

OP-AMP [V/div]	LPVT 1 [mV/div]	LPVT 2 [mV/div]	LPVT 3 [mV/div]	LPVT 4 [mV/div]
8.65	1.75	110	11.9	1.4

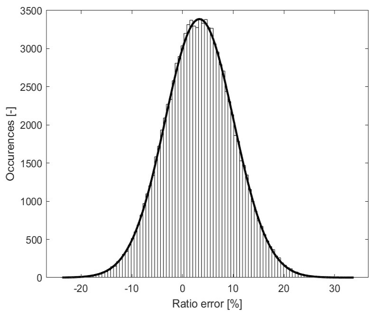

Fig. 12. PDF for ratio error at 150 kHz of LPVT 1

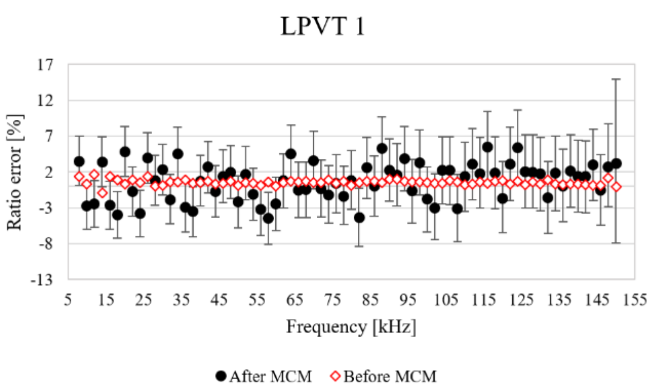

Fig. 13. Ratio error vs frequency of LPVT 1

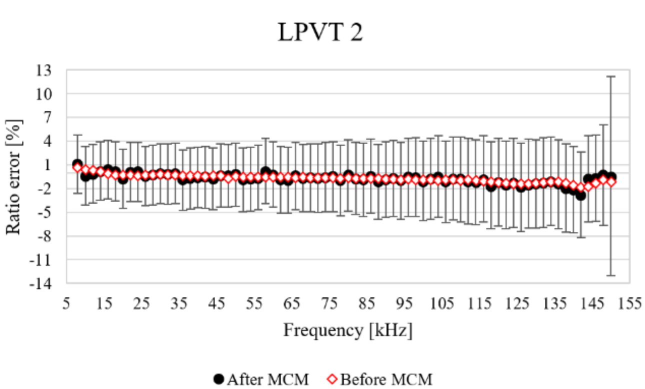

Fig. 14. Ratio error vs frequency of LPVT 2

attenuation of –0.02 dB, ensuring minimal distortion for this signal frequency.

$$H(f) = e^{-\frac{1}{2}\left(\frac{f}{f_c}\right)} \quad (4)$$

B. Uncertainty sources analysis

According to Fig. 1, the main source of uncertainty in the measurement setup is the oscilloscope. Therefore, the accuracy specifications of the scope, used to acquire the input and output of the sensors under test, are processed within the MCM method and Table VI collects the considered parameters. Reading error and full-scale error of Table VI are the accuracy parameters intended for DC measurements. However, in this article this DC specifications are used as first general indications to have a starting point to perform the uncertainty propagation process, since oscilloscope datasheets do not indicate accuracy parameters for AC measurements (based on the authors' knowledge). Instead, for AC conditions, the datasheet mentions the nominal vertical resolution of the ADC converter and the bandwidth. Finally, the vertical noise varies depending on how the vertical scale (in V/div) is set and Table VII shows the values used during testing for each measured signal.

C. MCM application

Once the sources of uncertainty are identified, the MCM can be implemented. In summary, this approach involves the distortion sample by sample of the acquired voltage waveforms, based on the accuracy parameters of the instrumentation outlined in Table VI. Since the shape of the probability density functions (PDFs) of these parameters are not known, it is assumed to be a rectangular distribution as suggested in standard [28]. In addition, since it is not possible to estimate the correlation of accuracy parameters on consecutive samples, to simplify the analysis, these parameters were considered as decorrelated. In conclusion, for all the DUTs, the ratio error, phase displacement and their 99 %-coverage intervals are calculated from 100000 Monte Carlo trials. Fig. 12 shows the ratio error output at 10 kHz for LPVT 1, and it highlights the Gaussian nature of the PDF. This behavior is common with all the other signals subjected to the MCM method corruption.

D. MCM results and discussion

In this paper, the MCM includes the uncertainty associated with the Type B evaluation associated with the proposed characterization method. For reasons of compactness and simplicity, the outputs of the MCM are presented graphically. For each DUTs (LPVT 1 – 4), for the range of frequency from 8 kHz to 150 kHz, Fig. 13 to 16 illustrate, with solid dots, the MCM results. The empty diamonds instead refer to the results shown in Fig. 3, added for the sake of clarity. Analogously, Fig. 18 to 21 use the same representation to depict the phase displacement results after the MCM implementation.

From the Fig. 13 – 16, for every frequency, the ratio error is presented with its 99 %-coverage interval. However, for all cases and all frequencies, the type A contribution is negligible and therefore not reported in the results of the Fig. 13 – 16. A note on LPVT 1 and 4, they show a higher variability especially at lower frequencies and then tend to stabilize. This behaviour could be attributed to the oscilloscope and to its accuracy parameters. In fact, according to the datasheet of the oscilloscope, the accuracy specifications of Table VI double in value if the vertical setting is lower to 1 mV/div, as is the case for LPVT 1 and 4 according to Table VII. On the contrary, LPVT 2 and 3, having a secondary output higher in value, have a lower dispersion.

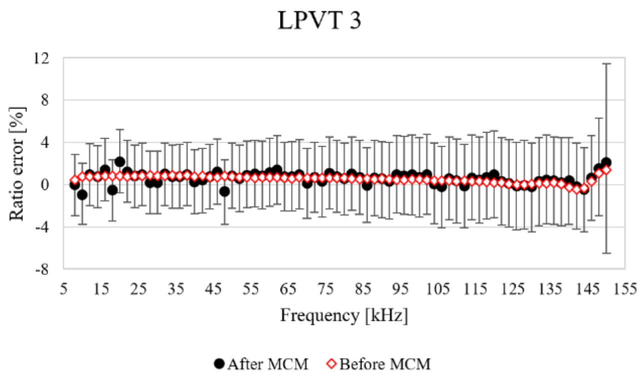

Fig. 15. Ratio error vs frequency of LPVT 3

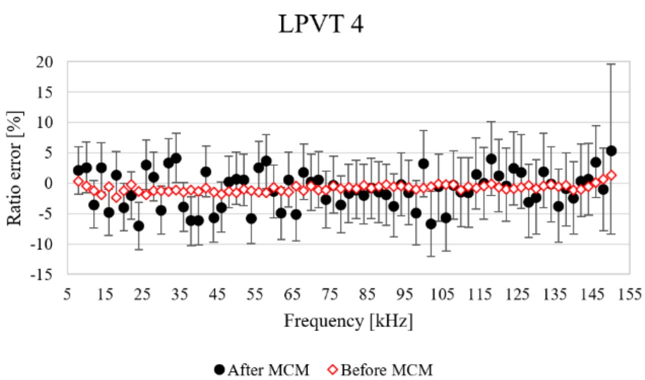

Fig. 16. Ratio error vs frequency of LPVT 4

Regarding the phase displacement displayed in Fig. 17 – 20, similar considerations can be expressed to those already made for the ratio error. However, in this case the 99%-coverage intervals do not always succeed in including the results obtained before the MCM.

Furthermore, the frequency dependency of the accuracy parameters was not removed or tackled at all because trivial in any measurement setup and out of the scope of the paper. As expected, as the frequency increases, so does the uncertainty interval.

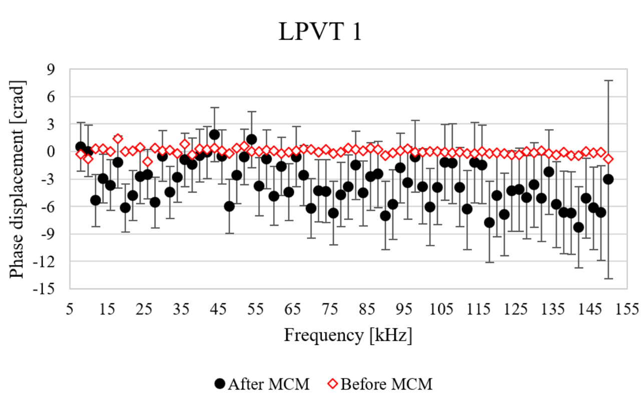

Fig. 17. Phase displacement vs frequency of LPVT 1

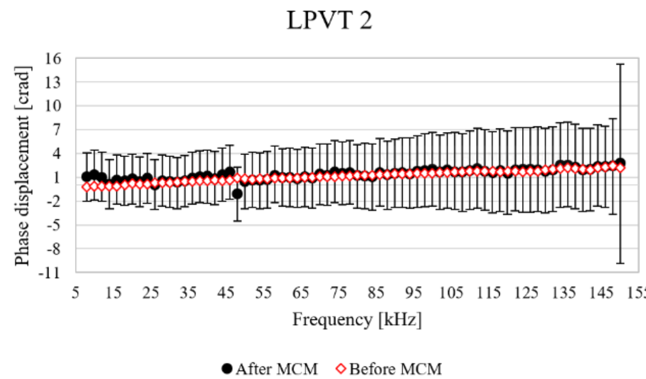

Fig. 18. Phase displacement vs frequency of LPVT 2

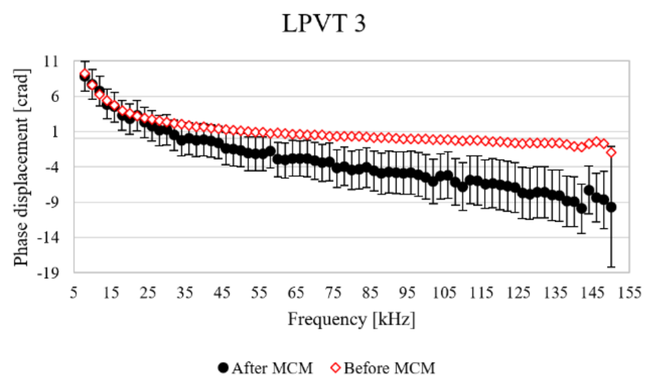

Fig. 19. Phase displacement vs frequency of LPVT 3

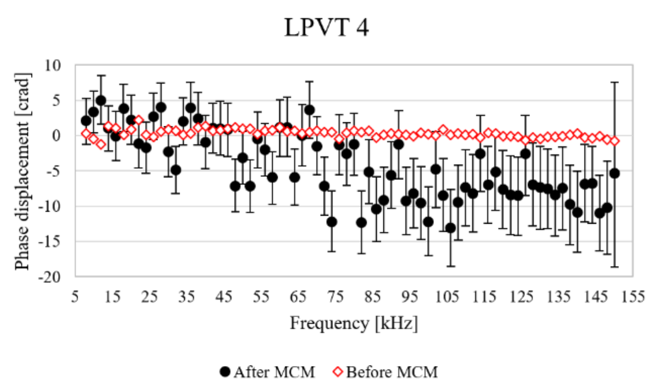

Fig. 20. Phase displacement vs frequency of LPVT 4

As a final comment regarding the uncertainty achieved by the method (i.e. the value of the coverage range extremes), often the maximum uncertainties calculated by the MCM far exceed the prescriptions of Table I. However, this is clearly due to the oscilloscope having worse accuracy parameters (Table VI) than the typical data acquisition board. Therefore, using more accurate, and therefore necessarily more expensive, instrumentation, smaller uncertainties would be obtained.

V. Conclusion

This paper, a technical extension of the study presented in [13], focuses on the uncertainty evaluation associated to the accuracy parameters obtained for the frequency range from 9 kHz to 150 kHz. Such an evaluation is applied to an innovative characterization of the frequency response of MV LPVTs. Currently, the extended frequency range of (9 to 150) kHz is under investigation. Given the lack of standard guidelines, a preliminary, fast, and straightforward characterization procedure was previously proposed. This work validates the proposed characterization method from a metrological perspective thanks to a comprehensive uncertainty assessment. To achieve this, Type A and B evaluation methods are applied, investigating the potential sources of uncertainty (not always clear/available to the user). The results demonstrate that this new frequency characterization method in the extended frequency range is effective and accurate in measuring the ratio error considering the instrumentation used (a reference oscilloscope) which makes its adoption suitable for all measurements laboratories involving preliminary tests on the ITs frequency response in the extended frequency range.

Acknowledgment

The project 22NRM06 ADMIT has received funding from the European Partnership on Metrology, co-financed by the European Union's Horizon Europe Research and Innovation Programme and from by the Participating State.

References

[1] Magesh T., Devi G., Lakshmanan T., Measurement and simulation of power quality issues in grid connected wind farms, (2022) Electric Power Systems Research, 210, art. no. 108142, DOI: 10.1016/j.epsr.2022.108142.

[2] Rajkumar S., Balasubramanian R., Kathirvelu P., A Comprehensive Review on Supraharmonics—The Next Big Power Quality Concern, (2024) Smart Grids and Sustainable Energy, 9 (1), art. no. 15, DOI: 10.1007/s40866-024-00195-4.

[3] J. Yaghoobi, A. Alduraibi, D. Martin, F. Zare, D. Eghbal, and R. Memisevic, 'Impact of high-frequency harmonics (0–9 kHz) generated by grid-connected inverters on distribution transformers', *International Journal of Electrical Power & Energy Systems*, vol. 122, p. 106177, Nov. 2020.

[4] Mariscotti A., Mingotti A., The Effects of Supraharmonic Distortion in MV and LV AC Grids, (2024) Sensors, 24 (8), art. no. 2465, DOI: 10.3390/s24082465.

[5] M. Kaczmarek, P. Kaczmarek, and E. Stano, 'The Reference Wideband Inductive Current Transformer', *Energies*, vol. 16, no. 21, Art. no. 21, Jan. 2023.

[6] R. Murray and J. A. de Kock, 'Evaluating Varying Burden when Inductive Current Transformers are Used for Harmonic Current Measurements', in *2023 IEEE 13th International Workshop on Applied Measurements for Power Systems (AMPS)*, Sep. 2023, pp. 01–06.

[7] G. Crotti *et al.*, 'Fast Frequency Characterization of Inductive Voltage Transformers Using Damped Oscillatory Waves', *IEEE Transactions on Instrumentation and Measurement*, vol. 73, pp. 1–14, 2024.

[8] Agazar M., Istrate D., Pradayrol P., Evaluation of the Accuracy and Frequency Response of Medium-Voltage Instrument Transformers under the Combined Influence Factors of Temperature and Vibration, (2023) Energies, 16 (13), art. no. 5012.

[9] P. S. Letizia *et al.*, 'Characterization of Instrument Transformers under Realistic Conditions: Impact of Single and Combined Influence Quantities on Their Wideband Behavior', *Sensors*, vol. 23, no. 18, 2023.

[10] Li Z., Xiang X., Hu T., Abu-Siada A., Li Z., Xu Y., An improved digital integral algorithm to enhance the measurement accuracy of Rogowski coil-based electronic transformers, (2020) International Journal of Electrical Power and Energy Systems, 118, art. no. 105806, DOI: 10.1016/j.ijepes.2019.105806.

[11] https://www.euramet.org/research-innovation/search-research-projects/details/project/measurement-methods-and-test-procedures-for-assessing-accuracy-of-instrument-transformers-for-power.

[12] https://www.euramet.org/research-innovation/search-research-projects/details/project/characterisation-of-ac-and-dc-mv-instrument-transformers-in-extended-frequency-range-up-to-150-khz.

[13] C. Betti, A. Mingotti, R. Tinarelli and L. Peretto, "A Low-Cost Measurement Setup to Test Low-Power Voltage Transformers in the 9 kHz - 150 kHz Frequency Range," *2024 IEEE 14th International Workshop on Applied Measurements for Power Systems (AMPS)*, Caserta, Italy, 2024, pp. 1-5, doi: 10.1109/AMPS62611.2024.10706688.

[14] Betti, C., Mingotti, A., Tinarelli, R., Peretto, L., Design of a Windowed Sinc for a Simplified Characterization of Low-Power Current Transformers, Paper presented at the I2MTC 2023 - 2023 IEEE International Instrumentation and Measurement Technology Conference, Proceedings, 2023-May, Kuala Lumpur.

[15] D.-E. Kim, G.-Y. Lee, G.-S. Kil, and S.-W. Kim, 'Trends in Measuring Instrument Transformers for Gas-Insulated Switchgears: A Review', *Energies*, vol. 17, no. 8, Art. no. 8, Jan. 2024.

[16] Mingotti A., Costa F., Peretto L., Tinarelli R., Accuracy Type Test for Rogowski Coils Subjected to Distorted Signals, Temperature, Humidity, and Position Variations, (2022) Sensors, 22 (4), art. no. 1397, DOI: 10.3390/s22041397.

[17] IEC 61869-1; Instrument Transformers—General Requirements for Instrument Transformers. IEC: Geneva, Switzwerland, 2023.

[18] IEC 61869-99; Instrument Transformers—Part 99: Glossary. IEC: Geneva, Switzerland, 2022.

[19] IEC-TR-61869-103; Instrument Transformers—The Use of Instrument Transformers for Power Quality Measurement. IEC: Geneva, Switzerland, 2012.

[20] IEC 61000-4-7; Electromagnetic Compatibility (EMC)–Part 4-7: Testing and Measurement Techniques–General Guide on Harmonics and Interharmonics Measurements and Instrumentation, for Power Supply Systems and Equipment Connected Thereto. IEC: Geneva, Switzerland, 2009.

[21] IEC 61000-4-30; Electromagnetic Compatibility (EMC)–Part 4-30: Testing and Measurement Techniques–Power Quality Measurement Methods. IEC: Geneva, Switzerland, 2015.

[22] IEEE-519; IEEE Recommended Practice and Requirements for Harmonic Control in Electric Power Systems. IEEE: New York, NY, USA, 2014.

[23] BS EN 50160:2010+A1; Voltage Characteristics of Electricity Supplied by Public Electricity Networks. BSI Standards Publication: London, UK, 2015.

[24] I. Dewayalage, D. A. Robinson, S. Elphick, and S. Perera, 'Measurement of High-Frequency Voltage Harmonics above 2 kHz in High-Voltage Networks', *Energies*, vol. 17, no. 4, Art. no. 4, Jan. 2024.

[25] G. Crotti *et al.*, 'Characterization of Voltage Transformers for MV Applications Up to 150 kHz - A Preliminary Study', in *2023 IEEE 13th International Workshop on Applied Measurements for Power Systems (AMPS)*, Sep. 2023, pp. 01–05.

[26] S. Schöttke, S. Rademacher, J. Meyer, and P. Schegner, 'Transfer characteristic of a MV/LV transformer in the frequency range between 2 kHz and 150 kHz', in *2015 IEEE International Symposium on Electromagnetic Compatibility (EMC)*, Aug. 2015.

[27] A. Mingotti, C. Betti, L. Peretto, and R. Tinarelli, 'Simplified and Low-Cost Characterization of Medium-Voltage Low-Power Voltage Transformers in the Power Quality Frequency Range', *Sensors*, vol. 22, no. 6, Art. no. 6, Jan. 2022.

[28] Supplement 1 BIPM JCGM 101:2008; Evaluation of Measurement Data—Supplement 1 to the Guide to the Expression of Uncertainty in Measurement—Propagation of Distributions Using a Monte Carlo Method. International Standardization Organization: Geneva, Switzerland, 2008.

[29] 'IEEE Standard for Digitizing Waveform Recorders', *IEEE Std 1057-2017 (Revision of IEEE Std 1057-2007)*, pp. 1–0, Jan. 2018.

[30] Evaluating Oscilloscope Bandwidths for Your Application, Keysight Technologies. https://www.keysight.com/us/en/assets/7018-01455/application-notes/5989-5733.pdf.